VIP *Wire Devices*

An Integrated "Energy Wire" for both Photoelectric Conversion and Energy Storage**

*Tao Chen, Longbin Qiu, Zhibin Yang, Zhenbo Cai, Jing Ren, Houpu Li, Huijuan Lin, Xuemei Sun, and Huisheng Peng**

The use of solar energy has the potential to provide an effective solution to the energy crisis.[1–5] Generally, the solar energy is converted into electric energy which is transferred through external electric wires to electrochemical devices, such as lithium ion batteries and supercapacitors, for storage.[6–13] To further improve the energy conversion and storage efficiency, it is important to simultaneously realize the two functions, photoelectric conversion (PC) and energy storage (ES), in one device. Recently, attempts have been made to directly stack a photovoltaic cell and a supercapacitor into one device which can absorb and store solar energy.[10–13] However, these stacked devices exhibited low overall photoelectric conversion and storage efficiencies. In addition, the planar format in such stacked devices has limited their applications, such as in electronic textiles where a wire structure is required.

Herein, an integrated energy wire has been developed to simultaneously realizes photoelectric conversion and energy storage with high efficiency. The fabrication is schematically shown in the Supporting Information, Figure S1. A titanium wire was modified in sections with aligned titania nanotubes on the surface. Active materials for photoelectric conversion and energy storage were then coated onto the modified parts with titania nanotubes. Aligned carbon nanotube (CNT) fibers were finally twisted with the modified Ti wire to produce the desired device. The Ti wire and CNT fiber had been used as electrodes. Figure 1a schematically shows a wire in which one part capable of photoelectric conversion and one part capable of energy storage. This novel wire device exhibits an overall photoelectric conversion and storage efficiency of 1.5%.

Aligned titania nanotubes were grown on the Ti wires by electrochemical anodization in a two-electrode system.[14] Figures 1b and 1c show typical scanning electron microscopy (SEM) images of titania nanotubes. The diameters of titania nanotubes ranged from 50 to 100 nm with the wall thickness varying from 15 to 50 nm, and their length was about 20 μm
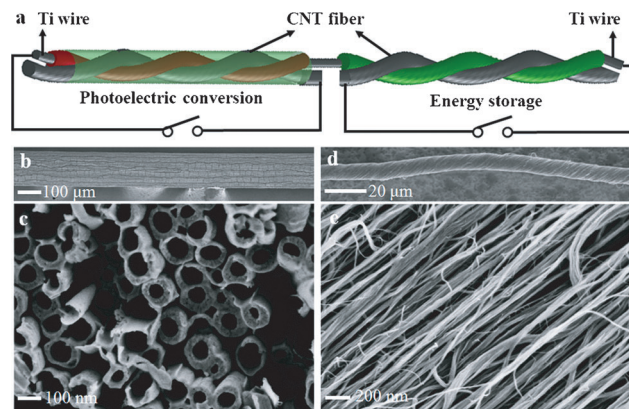

Figure 1. a) Schematic illustration of the integrated wire-shaped device for photoelectric conversion (PC) and energy storage (ES). b),c) Scanning electron microscopy (SEM) images of aligned titania nanotubes grown on a Ti wire by electrochemical anodization for 2 h at low and high magnifications, respectively. d),e) SEM images of a CNT fiber at low and high magnifications, respectively.

(Figure S2). In this case, titania nanotubes were mainly used to improve the charge separation and transport in photoelectric conversion and increase the surface area in energy storage.

Aligned CNT fibers were spun from spinnable CNT arrays which had been synthesized by chemical vapor deposition.[15–19] They could be produced with lengths of hundreds of meters through the continuous spinning process, and were typically ranged from 10 to 30 μm in diameter. Figure 1d shows a typical SEM image of a CNT fiber which has a uniform diameter of 10 μm. Figure 1e further shows that the CNTs are highly aligned in the fiber, which enables combined remarkable properties including tensile strength of 10^2–10^3 MPa, electrical conductivity of 10^3 S cm^{-1}, and high electrocatalytic activity comparable to the conventional platinum. In addition, the CNT fibers were flexible and could be easily and closely twisted with each other or with the other fiber materials (Figure S3), which was critical for the success in a wire-shaped device.

Photoactive materials were deposited onto the titania nanotube-modified parts on the Ti wire, for photoelectric conversion, while the desired gel electrolyte was coated onto the other sections for energy storage. Aligned CNT fibers were then twisted with both photoelectric-conversion and energy-storage parts to produce an integrated wire-shaped device. For simplicity, an "energy wire" which was composed of one photoelectric conversion section and one energy storage section had been mainly investigated in this work. Figure 2a shows a typical photograph of a wire with the left

[*] T. Chen, L. Qiu, Z. Yang, Z. Cai, J. Ren, H. Li, H. Lin, X. Sun, Prof. H. Peng
State Key Laboratory of Molecular Engineering of Polymers, Department of Macromolecular Science and Laboratory of Advanced Materials, Fudan University, Shanghai 200438 (China)
E-mail: penghs@fudan.edu.cn

© 2012 Wiley-VCH Verlag GmbH & Co. KGaA, Weinheim **WILEY** ONLINE LIBRARY **12143**
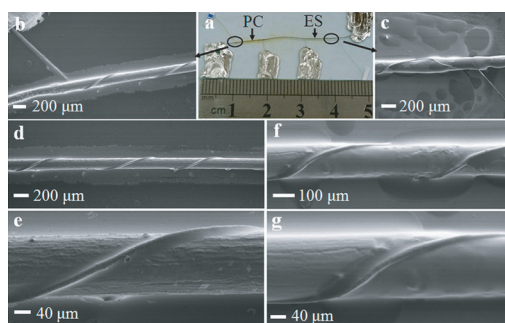
Figure 2. Structure characterization of an integrated energy wire. a) Photograph of a typical wire, see text for details. b) SEM image of an end PC part. c) SEM image of an end ES part. d,e) SEM images of the middle PC part at low and high magnifications. f,g) SEM images of the middle ES part at low and high magnifications.

8 mm for photoelectric conversion and the right 9 mm for energy storage. The ends of the Ti wire and CNT fibers were connected to external circuits for characterizations by indium (Figure 2b and c). Figure 2d and 2e indicate that the CNT fiber has been tightly contacted with the surface of the titania nanotubes, which is necessary for the success and high photoelectric conversion efficiency. The thread pitch of the CNT fiber around the Ti wire was about 1.1 mm. Similarly, the CNT fiber was also tightly twisted around the modified Ti wire with a thread pitch of about 0.7 mm in the energy-storage part (Figure 2f and g). The thread pitch could be tuned from 500 μm to 5 mm in both cases by varying the twisting parameter during the fabrication. Preliminary results showed that both photoelectric conversion and energy storage efficiencies increased with decreasing thread pitch. More efforts are underway along this direction. Herein the thread pitches of 1.1 and 0.7 mm for photoelectric-conversion and energy-storage parts, respectively, have been investigated.

The photo-harvesting material used in the photoelectric-conversion part was composed of *cis*-diisothiocyanato bis(2,2′-bipyridyl-4,4′-dicarboxylato) ruthenium(II) bis(tetra-butylammonium) (also called N719) as a dye and a solution of LiI, I₂, dimethyl-3-*n*-propylimidazolium iodide and 4-*tert*-butylpyridine in dehydrated acetonitrile as a redox electrolyte. N719 had been chemisorbed onto the titania nanotubes by immersing the modified Ti wire in a N719 solution, and the electrolyte was dropped onto the assembled CNT fiber and Ti wire after they had been twisted. The working mechanism is schematically shown in Figure 3a and further summarized as below. Electrons released when the dye molecules absorb sunlight are injected into the conduction band of titania nanotubes. The electrons are further transported to the Ti wire and reach the CNT fiber electrode by external circuit. Excited dye molecules are reduced to the ground state by I⁻ ions with production of I₃⁻ ions, which will be reduced to I⁻ ions by capturing electrons from the CNT fiber electrode.

The photovoltaic performance was measured under the illumination of AM 1.5 by recording the current-density/voltage (*J*–*V*) response. The effective area was calculated by multiplying the diameter and length of the photoelectric conversion part. The energy conversion efficiency ($\eta_{conversion}$)
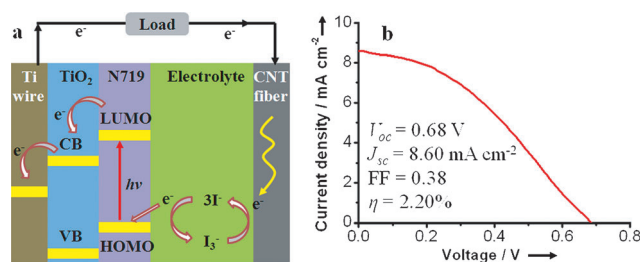

Figure 3. Characterization of the photoelectric conversion part. a) Schematic illustration to the working mechanism; CB = conduction band, VB = valence band. b) Typical current density/voltage curve under the illumination of AM 1.5.

was calculated by $\eta_{conversion} = FF\, V_{oc}\, J_{sc}/P_{in}$, where FF, V_{oc}, J_{sc}, and P_{in} correspond to fill factor, open-circuit voltage, short-circuit current density, and incident light power density (100 mW cm⁻² for AM 1.5), respectively. Figure 3b shows a typical *J*–*V* curve with FF, V_{oc}, and J_{sc} of 0.38, 0.68 V, and 8.60 mA cm⁻², respectively. The value of $\eta_{conversion}$ is calculated as 2.2%. The relative low FF may be derived from a poor contact between the CNT fiber and modified Ti wire, which can be improved by optimizing the twisting process and coating a thin layer of CNTs on the surface of CNT fiber. The photoelectric conversion efficiency of the photoelectric-conversion part could be also enhanced to 4% by increasing the length of the TiO₂ nanotubes.[14] Figure S4 shows the Nyquist plot of the photoelectric-conversion part: The left high-frequency semicircle corresponds to electron transport through the counterelectrode/electrolyte interface, indicating that I₃⁻ could be rapidly reduced to I⁻ catalyzed by CNTs to accelerate the diffusion of I₃⁻ ions.[20] The series ohm resistance (R_s) of this CNT fiber was high, which produced a low fill factor.

For the energy-storage part, the gel electrolyte containing poly(vinyl alcohol) and phosphoric acid in water was introduced between two electrodes. The electrochemical properties were characterized by cyclic voltammetry (CV) and the galvanostat method. Figure 4a shows CV curves with the increasing scan rate from 10 to 100 mV s⁻¹. The CV curves remained rectangular in shape for the different scan rates, indicating a high electrochemical stability and capacitance. Figure S5 shows a Nyquist plot of the energy-storage part: The vertical shape at low frequencies indicated a pure capacitive behavior, and the high series resistance was mainly derived from the CNT fiber electrode.[21] The specific
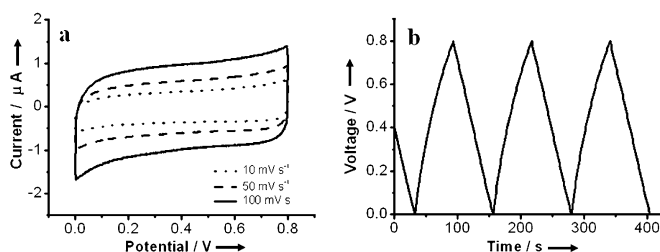

Figure 4. Characterization of the energy-storage part. a) Cyclic voltammetry curves at scan rates of 10, 50, and 100 mV s⁻¹. b) Charge–discharge curve at a current of 0.25 μA.

capacitance per unit length (C_L) was obtained from $C_L = I\Delta t/L\Delta V$, where I, Δt, L, and ΔV correspond to the current load (A), discharge time (s), cell length (cm) and potential window (V). Figure 4b shows a typical galvanostatic charge–discharge curve at a current of 0.25 µA. The value of C_L was calculated to be 0.024 mF cm^{-1}. Accordingly, the specific capacitance per unit area (C_S) was found to be about 0.6 mF cm^{-2} by $C_S = I\Delta t/S_{ES}\Delta V$ with S_{ES} as the surface area, which was calculated by multiplying the length and circumference of the Ti wire. Note that reported micro-supercapacitors typically show an area specific capacitance in the range of 0.4–2.0 mF cm^{-2},[22] indicating a good performance of the energy-storage part in our energy wire.

The energy wire would be charged upon exposure to the light when the photoelectric-conversion and energy-storage parts were connected (Figure 5a). The charging process of the
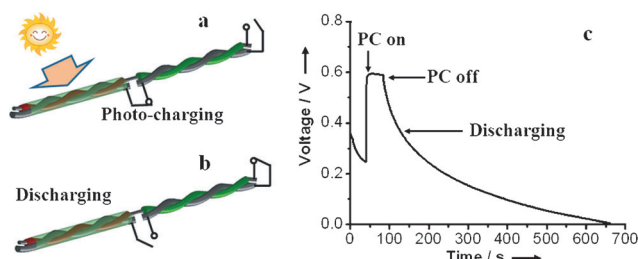

Figure 5. a, b) Schematic illustration of the circuit connection during charging and discharging processes, respectively. c) Photocharging–discharging curve of a typical energy wire. The discharging current is 0.1 µA.

integrated device under light illumination is shown in Figure S6. The negative and positive charges generated from the photoelectric-conversion part were transported towards the Ti wire and stored in and CNT fiber at the energy-storage part. The voltage–discharge measurement was conducted at a current of 0.1 µA when the photoelectric-conversion and energy-storage parts were disconnected (Figure 5b). The voltage change during the charging and discharging was carried out by connecting the energy-storage part with a potentiostat. Figure 5c shows the charge and discharge curves when the energy wire had been exposed to the light irradiation of AM 1.5 (100 mW cm^{-2}). Clearly, the voltage had been rapidly charged to 0.6 V upon the exposure to the light, which was close to, but a little lower than, the V_{oc} in the photoelectric-conversion part arising from self-discharge. The energy density in the energy-storage part (E_{ES}) was calculated to be 1.5×10^{-7} Wh cm^{-2} according to $E = 0.5 C_S V^2$, where V and C_S correspond to the operating voltage and specific capacitance, respectively. The energy-storage efficiency in the energy-storage part ($\eta_{storage}$) approaches to 68.4% based on $\eta_{storage} = E_{ES}S_{ES}/(P_{in}tS_{PC}*\eta_{conversion})$, where S_{ES}, t, P_{in}, S_{PC}, and η are the surface area of the energy-storage part, photocharging time illuminated light-energy density, effective area, and energy-conversion efficiency in the photoelectric-conversion part, respectively. The entire photoelectric conversion and storage efficiency was calculated to be about 1.5% by multiplying $\eta_{conversion}$ and $\eta_{storage}$. The integrated device was

flexible and could be bent without any obvious decrease in performance. As shown in Figure S7, the device parameters including energy-conversion efficiency, specific capacitance, and overall photoelectric-conversion and storage efficiency remained almost unchanged before and after bending.

It should be noted that the flexible and strong CNT fiber played a critical role on the effective realization of photoelectric conversion and energy storage in the energy wire. Other fiber materials, such as metal wires and modified polymer fibers coated with a conductive layer (e.g., indium tin oxide) on the surface, failed to make efficient devices under the same condition because of their relative mechanical instability. For instance, for a combined device of dye-sensitized solar cell and supercapacitor being fabricated on a modified polymethyl methacrylate fiber, showed an extremely low energy-conversion efficiency of 0.02% and area specific capacitance of 0.4 mF cm^{-2}.[22]

In conclusion, an integrated wire-shaped device has been developed to simultaneously realize both photoelectric conversion and energy storage. It exhibits a high overall photoelectric conversion and storage efficiency of 1.5%. The novel wire structure also enables unique and promising applications, for example, it is envisaged that it can be easily integrated into electronic textiles by a well-defined weaving technique and serve as a self-powering system for portable microelectronic devices and equipment.

Experimental Section

CNT fibers were spun from CNT arrays which had been synthesized by a typical chemical vapor deposition with Fe (1.2 nm)/Al$_2$O$_3$ (3 nm) on silicon wafer as the catalyst, ethylene as the carbon source, and a mixture of argon and hydrogen as the carrier gas.[14,15] Aligned titania nanotubes were grown on a Ti wire (diameter of 127 µm) by electrochemical anodization at 60 V for 2 h in a two-electrode system. A mixture of NH$_4$F (0.25 wt%) and H$_2$O (5 vol%) in ethylene glycol was used as the electrolyte, and the Ti wire and platinum plate were used as anode and cathode electrodes, respectively. After being washed by deionized water, the anodized Ti wire was annealed at 500°C in air for 1 h to produce the anatase titania.

Figure S1 schematically shows the fabrication of integrated wire devices, and the experimental details are summarized as below. 1) Aligned titania nanotubes were grown on the surface of a Ti wire. 2) The titania nanotubes at the middle and end were removed by using forceps with a sharp tip while the Ti wire was held by another forceps to produce two separate parts with one for PC and the other for ES. 3) 0.3 mM N719 solution in ethanol and *tert*-butyl alcohol with a volume ratio of 1/1 was coated onto one section of the aligned titania on the Ti wire to form the PC part at 120°C, and the resulting wire was maintained overnight at room temperature. 4) A gel electrolyte containing poly(vinyl alcohol) powder (10 g) and phosphoric acid (10 g) in water (100 mL) was then coated, by a dip-coating method, onto the second section of the aligned titania nanotubes on the Ti wire to form the ES part. 5) The modified Ti wire was fixed on a piece of glass, and CNT fibers were twisted round the two separate parts of the Ti wire. 6) The electrodes were connected to the external circuit with indium by an ultrasonic soldering mate (USM-V, Kuroda Techno), and the electrolyte containing 0.1 M LiI, 0.05 M I$_2$, 0.6 M dimethyl-3-*n*-propylimidazolium iodide, and 0.5 M 4-*tert*-butylpyridine in dehydrated acetonitrile was finally dropped onto the PC part.

The structures were characterized by SEM (Hitachi FE-SEM S-4800 operated at 1 kV) and TEM (JEOL JEM-2100F operated at 200 kV). The electrochemical characterizations were performed in

[1] B. O'Regan, M. Grätzel, *Nature* **1991**, *353*, 737 – 740.

[2] H. J. Snaith, L. Schmidt-Mende, *Adv. Mater.* **2007**, *19*, 3187 – 3200.

[3] N. S. Sariciftci, L. Smilowitz, A. J. Heeger, F. Wudl, *Science* **1992**, *258*, 1474 – 1476.

[4] B. C. Thompson, J. M. J. Fréchet, *Angew. Chem.* **2008**, *120*, 62 – 82; *Angew. Chem. Int. Ed.* **2008**, *47*, 58 – 77.

[5] M. Graetzel, R. A. J. Janssen, D. B. Mitzi, E. H. Sargent, *Nature* **2012**, *488*, 304 – 312.

[6] T. Miyasaka, T. N. Murakami, *Appl. Phys. Lett.* **2004**, *85*, 3932.

[7] T. N. Murakami, N. Kawashima, T. Miyasaka, *Chem. Commun.* **2005**, 3346 – 3348.

[8] T. Miyasaka, N. Ikeda, T. N. Murakami, K. Teshima, *Chem. Lett.* **2007**, *36*, 480 – 487.

[9] G. Dennler, S. Bereznev, D. Fichou, K. Holl, D. Ilic, R. Koeppe, M. Krebs, A. Labouret, C. Lungenschmied, A. Marchenko, D. Meissner, E. Mellikov, J. Méot, A. Meyer, T. Meyer, H. Neugebauer, A. Öpik, N. S. Sariciftci, S. Taillemite, T. Wöhrle, *Sol. Energy* **2007**, *81*, 947 – 957.

[10] C.-Y. Hsu, H.-W. Chen, K.-M. Lee, C.-W. Hu, K.-C. Ho, *J. Power Sources* **2010**, *195*, 6232 – 6238.

[11] H.-W. Chen, C.-Y. Hsu, J.-G. Chen, K.-M. Lee, C.-C. Wang, K.-C. Huang, K.-C. Ho, *J. Power Sources* **2010**, *195*, 6225 – 6231.

[12] G. Wee, T. Salim, Y. M. Lam, S. G. Mhaisalkar, M. Srinivasan, *Energy Environ. Sci.* **2011**, *4*, 413 – 416.

[13] W. Guo, S. Wang, C. Lin, Z. L. Wang, *Nano Lett.* **2012**, *12*, 2520 – 2523.

[14] T. Chen, L. Qiu, H. G. Kia, Z. Yang, H. Peng, *Adv. Mater.* **2012**, *24*, 4623 – 4628.

[15] X. Sun, W. Wang, L. Qiu, W. Guo, Y. Yu, H. Peng, *Angew. Chem.* **2012**, *124*, 8648 – 8652; *Angew. Chem. Int. Ed.* **2012**, *51*, 8520 – 8524.

[16] M. Zhang, K. R. Atkinson, R. H. Baughman, *Science* **2004**, *306*, 1358 – 1361.

[17] K. Jiang, Q. Li, S. Fan, *Nature* **2002**, *419*, 801.

[18] X. Zhang, Q. Li, T. G. Holesinger, P. N. Arendt, J. Huang, P. D. Kirven, T. G. Clapp, R. F. DePaula, X. Liao, Y. Zhao, L. Zheng, D. E. Peterson, Y. Zhu, *Adv. Mater.* **2007**, *19*, 4198 – 4201.

[19] H. Peng, X. Sun, F. Cai, X. Chen, Y. Zhu, G. Liao, D. Chen, Q. Li, Y. Lu, Y. Zhu, Q. Jia, *Nat. Nanotechnol.* **2009**, *4*, 738 – 741.

[20] E. Ramasamy, W. J. Lee, D. Y. Lee, J. S. Song, *Electrochem. Commun.* **2008**, *10*, 1087 – 1089.

[21] W. C. Chen, T. C. Wen, H. S. Teng, *Electrochim. Acta* **2003**, *48*, 641 – 649.

[22] J. Bae, Y. J. Park, M. Lee, S. N. Cha, Y. J. Choi, C. S. Lee, J. M. Kim, Z. L. Wang, *Adv. Mater.* **2011**, *23*, 3446 – 3449.